Unlocking the Day-side of Ultra-hot Jupiters: A NIR High-Resolution Emission Spectroscopy Study of WASP-33b

Stevanus K. Nugroho[1,2], Ernst de Mooij[3], Neale Gibson[4], Hajime Kawahara[5], Vivien Parmentier[6,7], Teruyuki Hirano[1,2,8], Masayuki Kuzuhara[1,2], Yui Kawashima[9], Matteo Brogi[10,11,12], Jayne Birkby[6], Takayuki Kotani[1,2,8], Kento Masuda[13], Christopher Watson[3], Konstanze Zwintz[14], Sayyed Ali Rafi[15], Motohide Tamura[15,1,2] & IRD Team

[1]Astrobiology Center, [2]National Astronomical Observatory of Japan, [3]Queen's University Belfast, [4]The University of Dublin, [5]ISAS/JAXA, [6]University of Oxford, [7]Laboratoire Lagrange, [8]The Graduate University for Advanced Studies (SOKENDAI), [9]RIKEN, [10]Università degli Studi di Torino, [11]University of Warwick, [12]INAF-Osservatorio Astrofisico di Torino, [13]Osaka University, [14]University of Innsbruck, [15]The University of Tokyo

Previously on the day-side of WASP-33b…

- WASP-33b is an ultra-hot Jupiter (T_{day}= 3290 K, De Mooij et al. 2013) orbiting a bright delta-scuti A-type star (T_{eff}= 7400 K, V= 8.3)
- Emissions of Fe I, Ti, I, V I, Si I, CO, & TiO are detected from its dayside suggesting a thermally inverted atmosphere (Nugroho et al. 2017, 2020, Herman et al. 2020, Serindag et al. 2021, Cont et al. 2021, 2022a, 2022b, Yan et al. 2022, van Sluijs et al. 2022)
- In Nugroho et al. (2021), using IRD/Subaru we detected the emission of OH+weak H_2O after the secondary eclipse as evidence of H_2O thermal dissociation (Lothringer et al. 2018, Parmentier et al. 2018)
- What about before the secondary eclipse?
- Is the H_2O signal real?

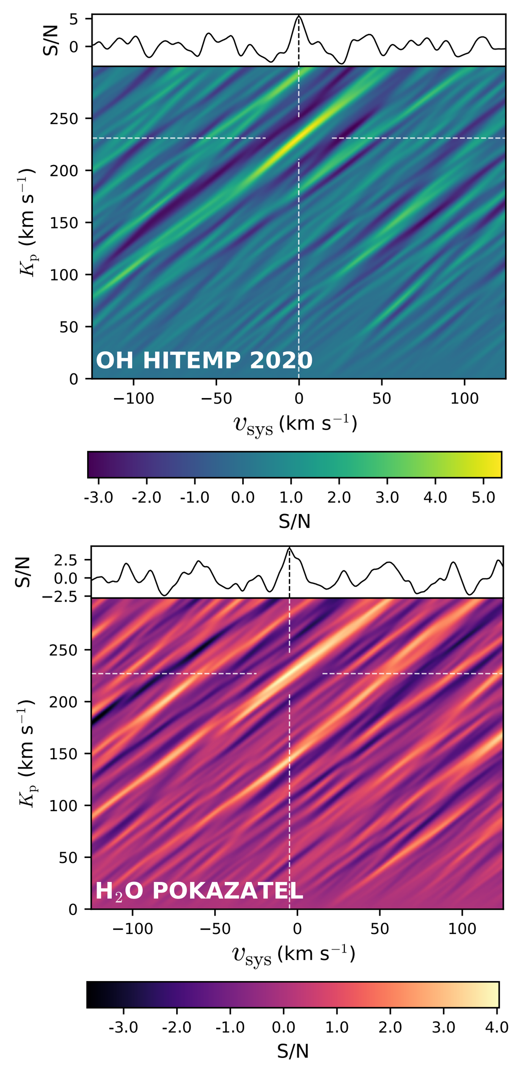

Direct fitting with HMC+NUTS (JAX+NumPyro)

Assuming constant abundances with altitude and the T-P profile from van Sluijs et al. (2022). Cross-sections are pre-calculated using Exojax 1.30 (Kawahara et al. 2022) and HELIOS-K 2.0 (Grimm et al. 2021). Models are preprocessed following Gibson et al. (2022).

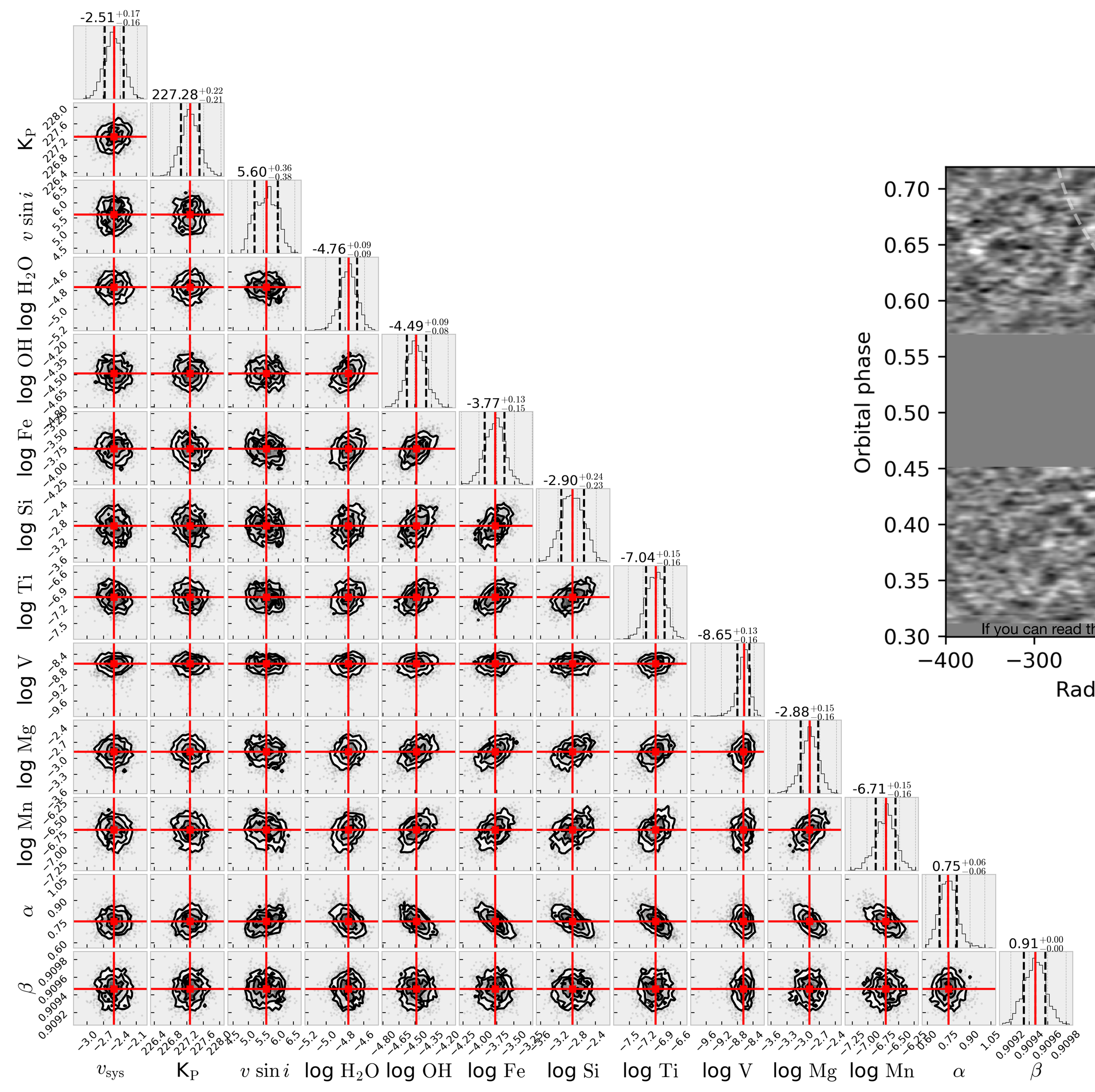

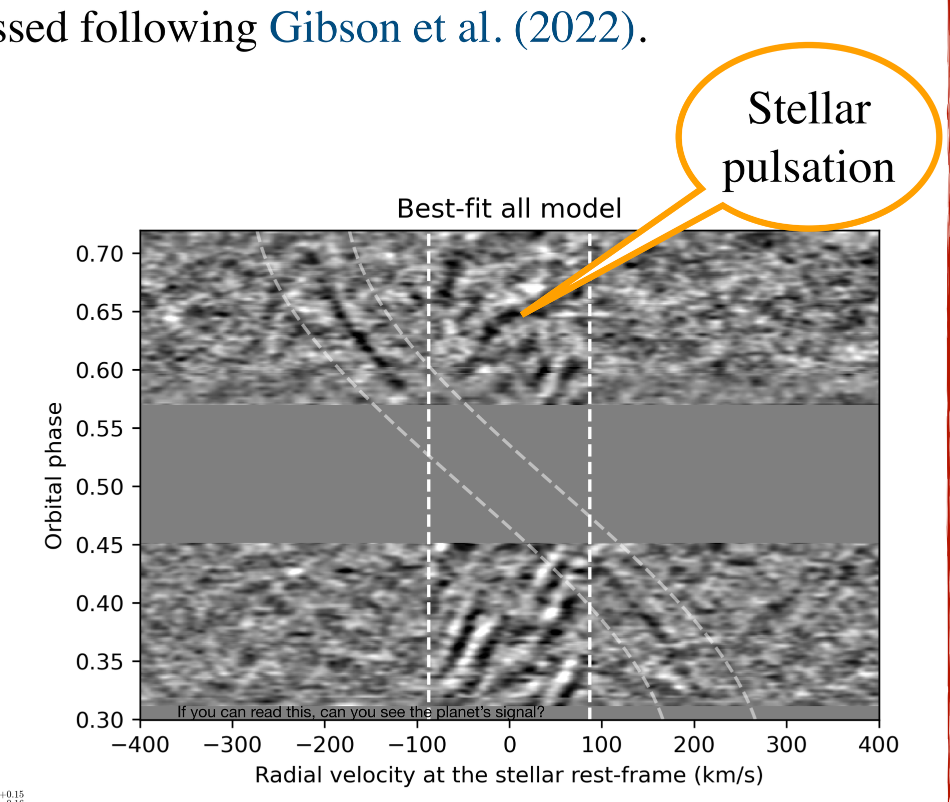

With the model constrained by this direct fitting, the planet's signal is detected at >30-sigma!

Follow up observations with IRD/Subaru

4 half-nights were awarded to S21B-11 (PI: Nugroho) allowing us to observe 2 half-nights before and 2 half-nights after the secondary eclipse using IRD (R~70,000; YJH-bands)

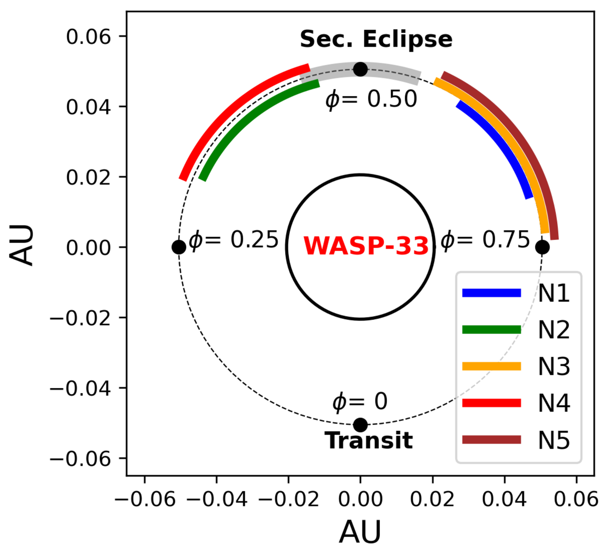

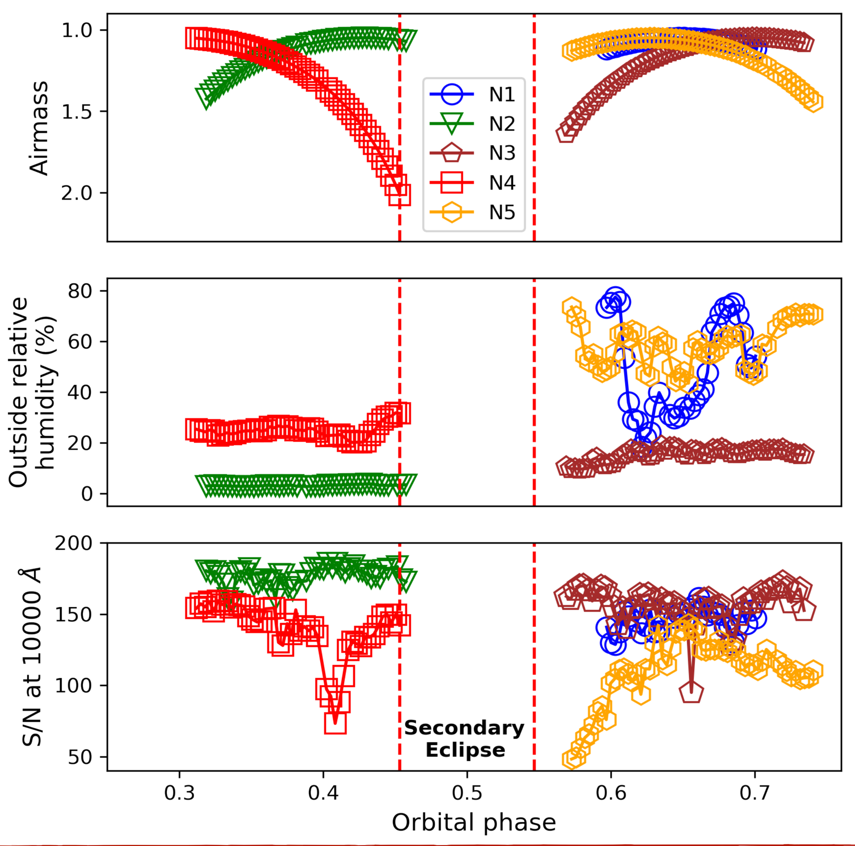

Analysis of symmetric orbital phase coverage

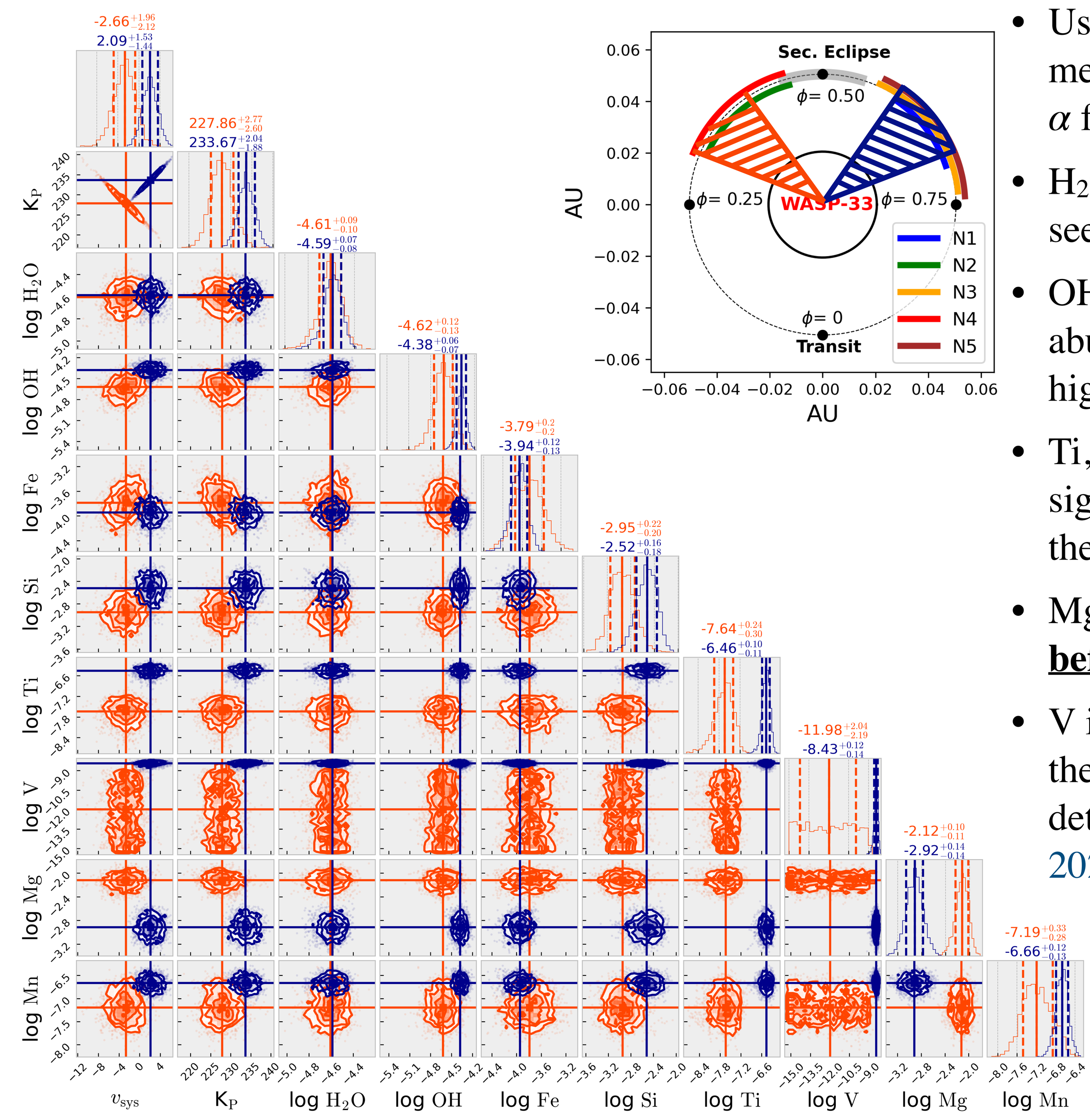

- Using a fixed T-P, and the median of the v sin i, and α from the above analysis
- H_2O and Fe abundance seem homogenous
- OH, Si, and Mn abundances are a bit higher **after** the eclipse
- Ti, V abundances are significantly higher **after** the eclipse
- Mg abundance is higher **before** the eclipse
- V is detected only after the eclipse? It was detected by Cont et al. 2022

Post-processings & stopping SysRem

- The stellar & telluric lines using an iterative detrending algorithm, SysRem (Tamuz et al. 2005), leaving the Doppler-shifted planetary lines more/less intact while the temporally static stellar and telluric lines were removed.
- Then how to stop the iteration? The idea is to observe the gradient RMS (or ΔRMS) of the "residuals". Stop the SysRem as soon as the trend doesn't significantly change, and check if the telluric has been successfully removed.

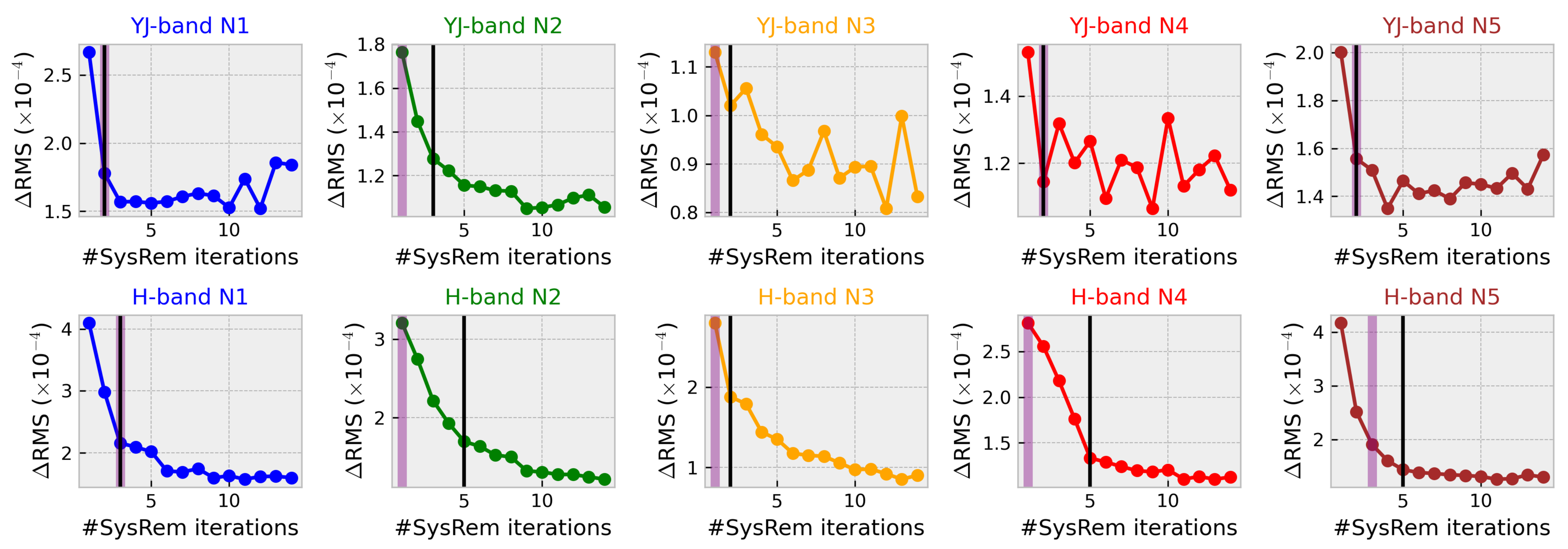

- The above are the ΔRMS of each band of each data-sets as a function of #SysRem iterations, the vertical black line is where the iteration was stopped, while the vertical purple line indicates when the CCF telluric is ~3 sigma of the noise.

Chemical phase-curves

Previously, we introduced a scale factor of the model's line-contrast as a function of the orbital phase (see poster by Ernst de Mooij, Herman et al. 2022). Here, inspired by Hoeijmakers et al. (2022), we added a squeezing factor (i.e. exponential constant) to account for a possible localisation of the signal on the day-side of the planet.

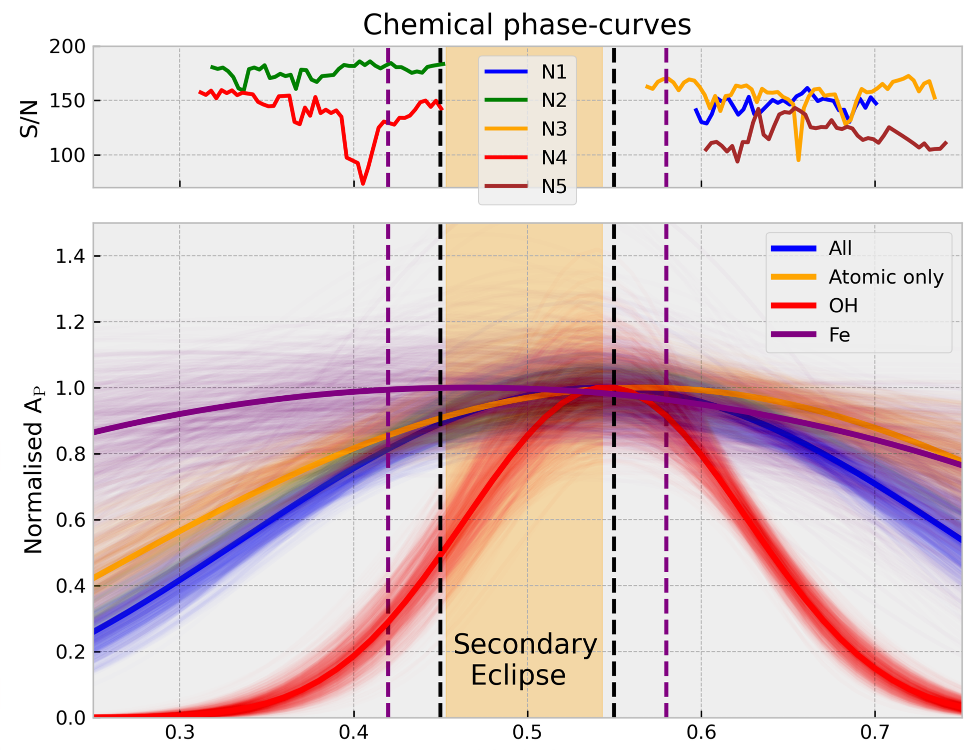

$$\mathcal{L}(\Theta) = \prod_{i=1}^{N} \frac{1}{\sqrt{2\pi(\beta\sigma_i)^2}} \exp\left(-\frac{1}{2}\frac{(f_i - A_p(\alpha,\phi,\gamma)m_i(\Theta))^2}{(\beta\sigma_i)^2}\right)$$

$$A_p(\alpha,\phi,\gamma) = \alpha\left(1-\cos^2(\pi(\phi-\theta))\right)^{\gamma}$$

- The peak of all species, atomic species only, & OH only is shifted toward after the eclipse by ~$15.32^{+3.80}_{-2.97}$, $23.80^{+12.77}_{-7.05}$, & $16.36^{+2.24}_{-2.17}$ degree, respectively, consistent with Herman et al. (2022). However, we couldn't get a tight constraint for Fe from our IRD data alone ($-11.99^{+24.63}_{-35.61}$ degree).
- Notice that the OH "phase-curve" is more squeezed than others suggesting it originates from a localised area on the day-side
- Need a 3D atmospheric model?

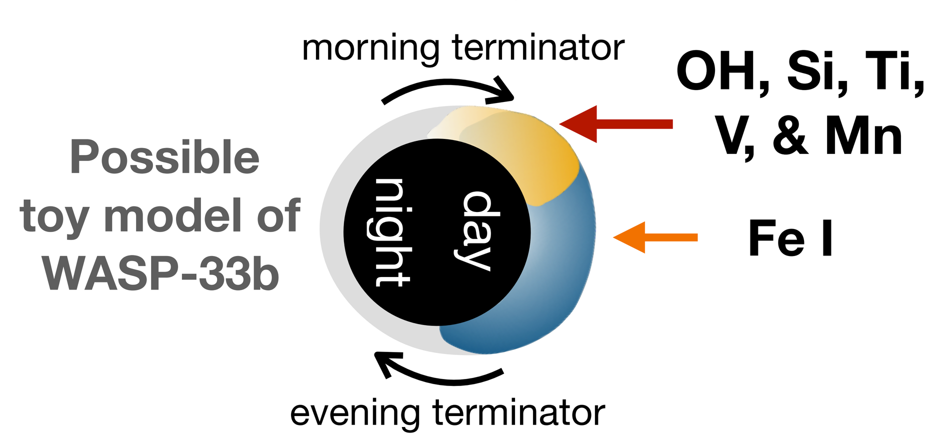

Detection of Mg I and Mn I & confirmation of OH, Fe I, Si I, & Ti I

No or weak H_2O?

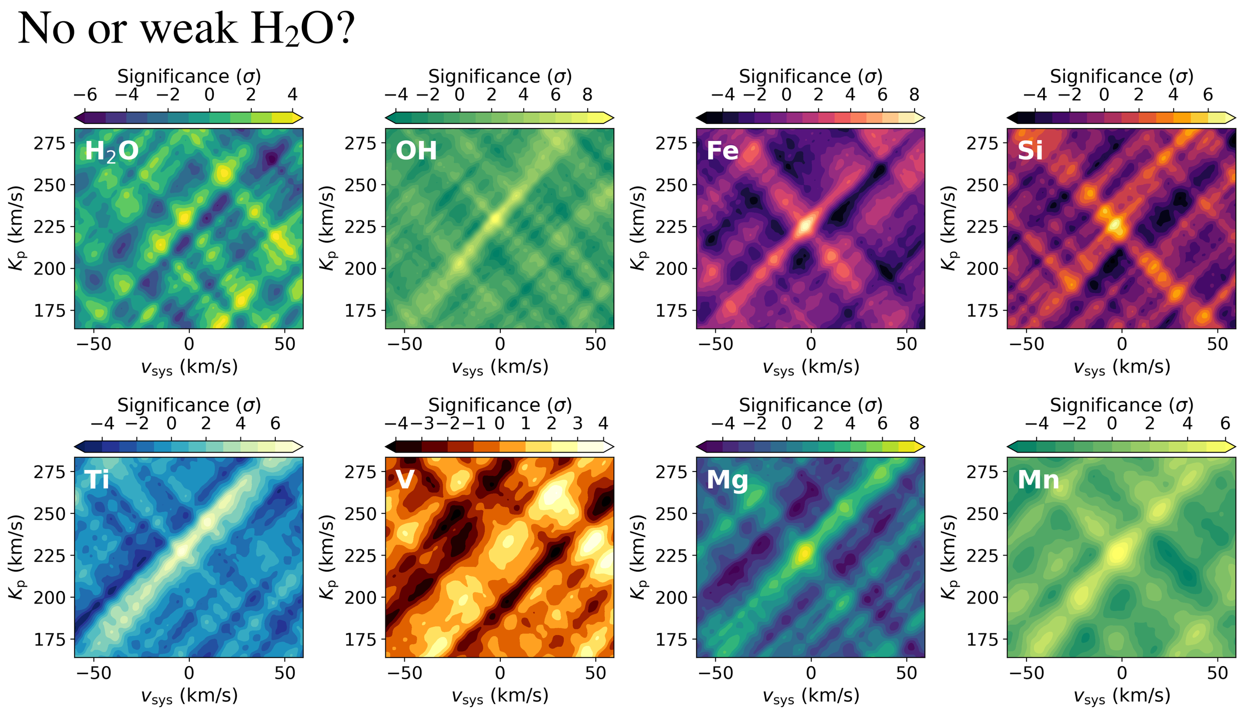

- Assuming chemical equilibrium and T-P profile from van Sluijs et al. 2022
- Produced using the "alpha significance method" via likelihood mapping (Gibson et al. 2020) as it is hard to sample properly (WASP-33 is a pulsating star) the noise using the "Kp-Vsys map method".

To be continued…